Observation of Nonlinear Self-Trapping of Broad Beams in Defocusing Waveguide Arrays

Francis H. Bennet,[1] Tristram J. Alexander,[1,2] Franz Haslinger,[1] Arnan Mitchell,[3] Dragomir N. Neshev,[1] and Yuri S. Kivshar[1]

[1]*Nonlinear Physics Centre, Centre for Ultrahigh-Bandwidth Devices for Optical Systems (CUDOS), Research School of Physics and Engineering, Australian National University, Canberra, ACT 0200 Australia*
[2]*School of Physical, Environmental and Mathematical Sciences, UNSW@ADFA, Canberra ACT 2600, Australia*
[3]*CUDOS, School of Electrical and Computer Engineering, RMIT University, Melbourne Vic 3001, Australia*

(Received 7 November 2010; revised manuscript received 6 January 2011; published 28 February 2011)

We demonstrate experimentally the localization of broad optical beams in periodic arrays of optical waveguides with defocusing nonlinearity. This observation in optics is linked to nonlinear self-trapping of Bose-Einstein-condensed atoms in stationary periodic potentials being associated with the generation of truncated nonlinear Bloch states, existing in the gaps of the linear transmission spectrum. We reveal that unlike gap solitons, these novel localized states can have an arbitrary width defined solely by the size of the input beam while independent of nonlinearity.

DOI: 10.1103/PhysRevLett.106.093901 PACS numbers: 42.70.Qs, 03.75.Lm, 42.65.Jx, 42.65.Tg

The coherent transport of nonlinear waves is essential in many phenomena in nature. In contrast to linear waves, the physics becomes complex when wave interactions start to play a role, making laboratory studies difficult. As such, many of the fundamental physical effects of nonlinear waves have been first studied in optics, where the advent of the laser as an intense coherent light source gave rise to the field of nonlinear optics. The recent experimental developments in Bose-Einstein condensates (BECs) opened the way for many analogous experiments with intense sources of coherent matter waves. Correspondingly, many effects earlier observed in nonlinear optics have been later found to occur in nonlinear atom optics, including four-wave mixing of matter waves [1] and matter-wave solitons [2].

A few years ago Anker *et al.* [3] reported the experimental observation of nonlinear self-trapping of Bose-Einstein-condensed atoms in stationary periodic potentials. This trapping effect due to interaction between condensed atoms is manifested as a change from the diffusive regime, characterized by an expansion of the condensate, to the nonlinearity dominated self-trapping regime, where the initial expansion stops and the width of a matter-wave packet remains finite. This observation abrogates a seemingly obvious analogy between nonlinear optics and matter-wave physics, because this type of nonlinearity-induced self-trapping in the presence of *repulsive interaction* has never been observed in optics.

In this Letter, we report on the first observation of nonlinear self-trapping of broad beams with zero transverse momentum in an array of defocusing optical waveguides. Our results not only provide an optical analogue of the self-trapping effect of Bose-Einstein-condensed atoms [3], but also reveal the important unique features of these localized states. In particular, we demonstrate that unlike conventional gap solitons known in defocusing photonic lattices [4] and BECs [5], the spatial extent of such self-trapped states is controlled by the width of the input excitation rather than by the input power.

While a detailed intuitive explanation of the self-trapping effect in terms of wave tunneling in a single Josephson junction has been provided in Ref. [3], this description was found incomplete as it did not account for the periodic nature of the trapping potential. Subsequent theoretical works [6–8] have extended the description of the wave localization linking it to the Bloch modes in the system. However, this subsequent description remained untested experimentally, largely due to the challenges in BEC experiments. By using an optical system, here we investigate the nature of the self-trapped state to a degree not attainable in the original BEC system. As such, we demonstrate experimentally *two new fundamental effects*: (i) Dependence of the width of the localized state on the input excitation, and (ii) independence of the localization on the strength of the nonlinearity (beam power, or equivalently number of atoms in the BEC system), once above a critical value. This is due to the existence of a class of robust nonlinear states with arbitrary width which act as attractors in the system. Loss of excess power (or equivalently atoms) is able to occur through the edges of the localized state [7], an effect unnoticed in the earlier experiments due to the deep lattice used. We reveal that the unique properties of the self-trapped states make them both highly robust and easily controllable.

We begin with the theoretical description of the beam localization, and model beam propagation through our lithium niobate ($LiNbO_3$) waveguide array by the nonlinear Schrödinger equation with a periodic potential and Kerr-type nonlinearity,

$$i\frac{\partial E}{\partial z} + D\frac{\partial^2 E}{\partial x^2} + \rho\Delta n(x)E - \gamma|E|^2E = 0. \qquad (1)$$

Here $D = z_s\lambda/(4\pi n_0 x_s^2)$, $\rho = 2\pi z_s/\lambda$. The transverse coordinate x and longitudinal coordinate z are normalized in units of $x_s = 1$ μm and $z_s = 1$ mm, respectively. While the complete description of the defocusing photovoltaic nonlinearity of $LiNbO_3$ involves complex charge diffusion processes, our simplified model captures well the generic features of the nonlinear beam evolution, as was successfully demonstrated for gap solitons in Ref. [9]. The linear refractive index of the substrate material is $n_0 = 2.234$ at $\lambda = 532$ nm, leading to a diffraction coefficient of $D = 18.95$. The linear refractive index change $\Delta n(x)$ of the waveguides is taken as $\Delta n(x) = \epsilon\sum_n \exp[-(x - nd)^2/w^2]$, where ϵ defines the modulation depth [4]. We take the waveguide width and spacing to be $w = 7$ μm and $d = 14$ μm respectively, matching the experimental realization of the array. The modulation depth is set at $\epsilon = 0.0003$ to match the theoretical and experimental linear output profiles. This is a shallow depth compared to the experimental regime of Ref. [3]. We find however that the general effects presented in this work occur over a wide range of depths ($\epsilon = 0.0002$–0.005 have been considered).

We examine the stationary solutions of the system Eq. (1) using the ansatz $E(x, z) = \phi(x)\exp(i\beta z)$, where β is the propagation constant (related to the negative value of the chemical potential in BEC physics). In the linear limit the stationary wave solutions take the form of Bloch waves, $\phi_{n,k}(x) = U(x)\exp(ikx)$ where n denotes the band number and k the Bloch wave vector. The spectrum of these linear waves is divided into bands separated by gaps as shown in Fig. 1(a). In the presence of nonlinearity, stationary solutions may exist inside the linear transmission gaps in the form of either periodic nonlinear Bloch waves [10] or spatially localized states known as gap solitons [11]. A third type of state has recently been revealed as a bridge between these two classes of solution, the so-called *truncated nonlinear Bloch waves* [6]. Such a type of localization occurs when the propagation constant of the Bloch wave is shifted into the gap, passing through the entire linear band, as shown with an arrow in Fig. 1(a). This crossing happens when a Bloch wave with zero transverse momentum is excited at the top of the first band and the defocusing nonlinearity decreases the propagation constant into the Bragg reflection gap. Intuitively this can be understood as confining a truncated piece of the Bloch wave between two Bragg reflectors, with no radiation into other linear waves due to the presence of the linear band gap. Unlike conventional gap solitons in defocusing lattices, where the width of the soliton is proportional to the soliton power [11], the width of the truncated state is a control variable [8] in the sense that it selects the soliton family out of an infinite number of families (for an infinite lattice), each with a different number of occupied lattice sites. The particular family excited depends on the initial width of the incident optical beam. The families are all distinct, bifurcating near the upper gap edge above a critical value of the nonlinear Bloch wave intensity [6,8]. Two particular examples of truncated nonlinear Bloch waves of different widths are shown in Figs. 1(b) and 1(c). Such localized states can also be regarded as multisoliton states [12], but stable even when composed of many gap solitons.

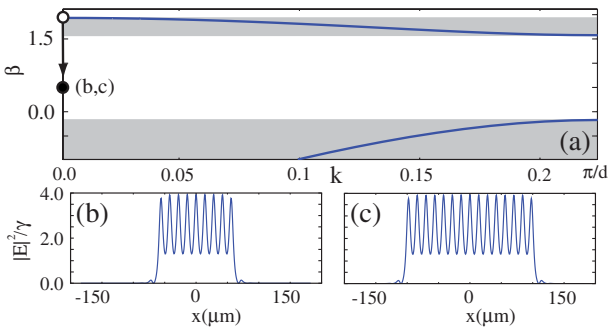

FIG. 1 (color online). (a) Band-gap spectrum. (b),(c) Examples of two truncated nonlinear Bloch waves of different widths.

Next we examine the excitation of such localized Bloch waves from a Gaussian input. Figure 2 summarizes the numerical results on the Bloch wave excitation for different values of the optical nonlinearity. As shown in Fig. 2(a), for weak defocusing nonlinearity the beam undergoes rapid spreading (faster than linear diffraction). However as the nonlinearity is increased this spreading is suddenly halted and the beam localizes with a width of the order of the width of the input beam. As is evident in a comparison of Figs. 2(b) and 2(c) the signature of the truncated nonlinear Bloch wave is the sharp intensity drop-off in the wings of the beam. Additional features visible in Figs. 2(a) and 2(b) are the strong intensity modulations occurring within the localized state. The large diffraction

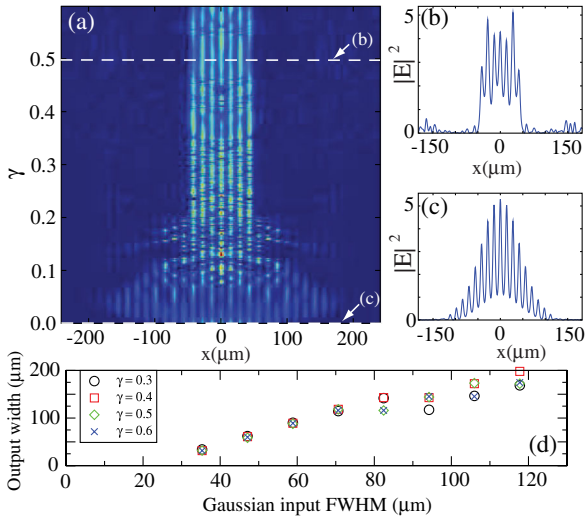

FIG. 2 (color online). (a) Dependence of the output intensity profile on the nonlinearity γ. The beam spreading is arrested at a critical nonlinearity, $\gamma \approx 0.15$. (b),(c) Output beam profiles [as marked in (a)] showing localization. (d) Variation of the output beamwidth (defined as the width between the sharp boundaries) with the input beam full width at half maximum (FWHM) for different values of the nonlinear coefficient γ.

coefficient leads to long-lived nonlinear excitations of the truncated nonlinear Bloch wave, which despite the strong modifications of the intensity profile do not lead to decay of the localized state. Most importantly, Fig. 2(a) shows that above a certain threshold for the optical nonlinearity ($\gamma \approx 0.15$), the width of the localized state remains practically independent of the input beam power.

Interestingly, the localization occurs even when the nonlinearity is strong enough to detune the propagation constant of the beam into the higher band. The localization in this latter case occurs through a rapid loss of power from the central part of the beam into higher-order low intensity nonlinear Bloch waves, effectively moving the propagation constant back into the linear gap [6]. This is an important feature not addressed in the earlier experiments using deep lattices [3]. It is also in contrast to the long-lived nonlinear excitations of the Bloch wave background [13].

An important feature of the generation process is that the output beamwidth is solely defined by the input width of the Gaussian beam, while being independent of the medium's nonlinearity. There is a linear dependence [Fig. 2(d)] between the input and output widths, while the different values of the nonlinearity lead to identical output beamwidths. This can be understood as a consequence of the requirement of a critical intensity for generation [6]. As the nonlinearity (or beam power) is increased, the number of excited waveguides above the critical intensity does not change for moderate beamwidths. At larger beamwidths the nonlinear excitations of the truncated nonlinear Bloch state may lead to fluctuations in the measured width. This behavior arises due to the existence of independent families of arbitrary, but fixed, width which persist even into the higher-order bands (where radiation occurs). Increasing the power of such states changes the maximum intensity, but not the width. Stable nonlinear localized states with arbitrary fixed widths have not been seen before in any physical context, and the existence of these nonlinear states as stable attractors is at the heart of the new results of this work.

Experimentally, we test the excitation of truncated Bloch waves by employing the defocusing nonlinearity of a $LiNbO_3$ waveguide array (6 cm long, fabricated by titanium indiffusion). Because of the slow nature of the photovoltaic nonlinear response in $LiNbO_3$, the nonlinear index change increases slowly with time under a constant input laser power. Since the time scale of this index change is of the order of several minutes, the time dependence of the beam output intensity profile can be mapped to the dependence on the nonlinear coefficient γ in Eq. (1). The dependence $\gamma(t)$ is a nonlinear function that saturates at large times, however, it is a monotonic function and uniquely defines the nonlinear index change.

We excite the array with a broad Gaussian laser beam at 532 nm. The input beam [Fig. 3(a)] is elliptically shaped by a cylindrical lens ($f = 50$ mm) before a ($20\times$) focusing objective. We monitor the beam output intensity profile with time for a typical input power of 1 mW and measure

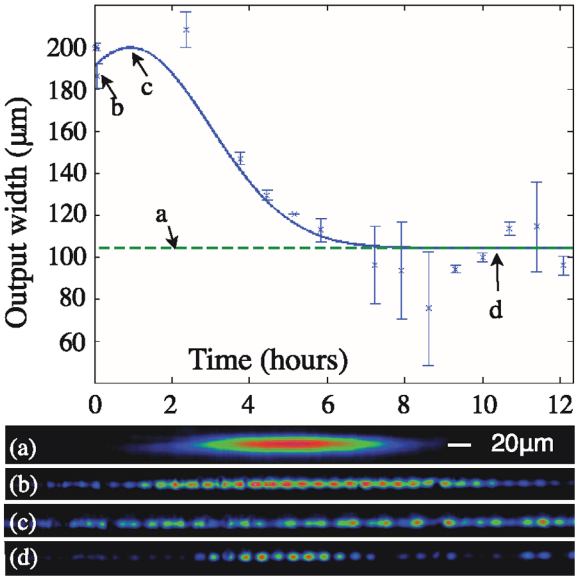

FIG. 3 (color online). Output beamwidth (estimated as the width containing 50% of the total light) vs time (nonlinear index change). Dashed line—the width of 75% of the input beam. (a) Input beam profile; (b) linear diffraction at the output. (c) Nonlinear defocusing at low nonlinearity (time), (d) beam localization at high nonlinearity. Beam power, 1 mW.

the variation of the beamwidth. We note that at these laser powers we are far from nonlinearity saturation with intensity [9]. The width of the output beam (Fig. 3) is determined as the size of the area which contains 50% of the output light power. This allows us to filter out any noise in the diffraction pattern while maintaining a high degree of accuracy. Error bars are calculated as the asymmetry of the output profile with respect to the center of the input beam.

The linear diffraction in the array causes the beam to spread out and occupy nearly twice the number of waveguides in comparison to the input beam [Fig. 3(b)]. Upon increase of the nonlinearity with time, we observe an initial defocusing of the beam [(c)] resulting from the weak negative nonlinearity. As the exposure time increases and the nonlinearity grows, the beam experiences gradual confinement and reduces its width [(d)]. The dependence of the beamwidth with time is plotted in the main panel of Fig. 3, where we observe that the beam localizes and the width remains essentially constant. This localized state has a width equal to the width of the input beam containing 75% of the power, where the remaining 25% has been lost in radiation. Small oscillations around this value are observed at longer times, thus matching the numerical predictions in Fig. 2.

The appearance of spatial frequencies at the edges of the Brillouin zone is proof that the nonlinear localization is inside the Bragg reflection gap. This is seen in the insets of Fig. 4 together with the intensity profiles of the beam for linear and nonlinear propagation. We note that the intensity scale in the Fourier spectrum plots is nonlinear due to the nonlinear response of the camera.

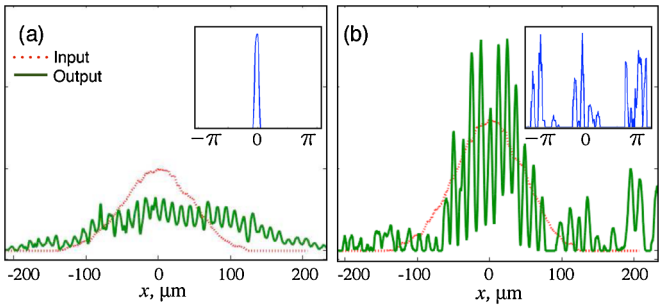

FIG. 4 (color online). Beam profiles at the array input (dotted line) and output (solid line) for (a) linear ($t \sim 0$) and (b) nonlinear ($t = 10$ hours) propagation, corresponding to Figs. 3(b) and 3(d). Insets: Fourier spectrum of the output beams. $\pm\pi$ indicate the edges of the Brillouin zone of the lattice.

A unique property of the optical system is the ability to control independently the width and the power of the input beam. This control allows us to test the new feature of nonlinear Bloch wave localization—that it is parameterized by the input beamwidth rather than by the input power. For this purpose the input beamwidth in our experiment is reduced using a cylindrical lens with $f = 75$ mm. This arrangement results in an input beam nearly half the beamwidth in Fig. 3(a). The variations of the output beamwidth vs the increase of the nonlinear response with time is shown in Fig. 5. Because of the strong diffraction in this case, the output beam profile acquires more noise and we therefore estimate the beamwidth as the area containing 30% of the total output power. Nevertheless, we can again identify similar behavior of the output beam evolution.

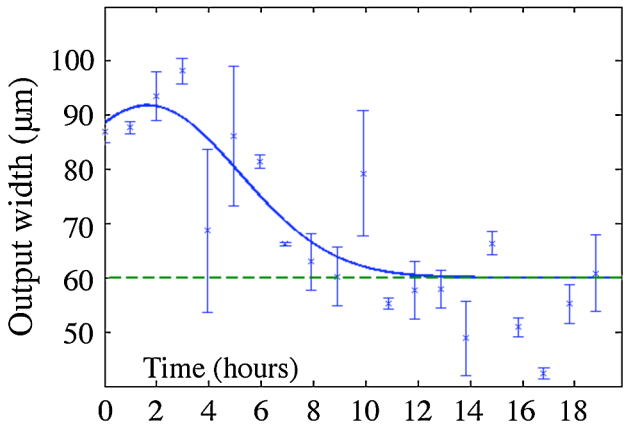

FIG. 5 (color online). Output beamwidth (estimated as the width containing 30% of the total light) vs time (nonlinear index change). Dashed line indicates the width of 65% of the input beam. Beam power, 1 mW.

First we observe the initial beam defocusing with increase of the nonlinearity, while at longer times the beam confines to a narrower localized state equal to the width of the input beam containing about 65% of the total input power.

The higher loss in this localization process can be intuitively understood since the narrower beam (of the same power) used in Fig. 5 has approximately twice higher intensity than the beam of Fig. 3. This higher intensity pushes the propagation constant into the higher-order bands, leading to higher losses. Most importantly, however, the experiments shown in Figs. 3 and 5, confirm the unique property of the truncated Bloch wave localization in comparison to any other nonlinear localized states known in nature, namely, that the width of the localized state remains independent of the nonlinearity, but can be chosen by the width of the input excitation.

In conclusion, we have observed nonlinear self-trapping of broad optical beams in defocusing waveguide arrays. We have revealed that these novel types of spatially localized modes can have an arbitrary width defined by the input beam, while the width is practically independent of nonlinearity. The origin of these effects lies in the existence of an infinite number of independent families of localized solutions with different, but fixed, widths, which persist into the higher-order bands of the linear band-gap structure. Our experimental results provide the first proof of the existence of the unique properties of such states. We believe that the robust nature of the truncated nonlinear Bloch states and their controllable generation will encourage their observation in other physical systems, including higher dimensional ones.

We thank V. Konotop, E. Ostrovskaya, J. Yang, and A. Truscott for useful discussions, and acknowledge financial support from the Australian Research Council.

[1] L. Deng *et al.*, Nature (London) **398**, 218 (1999).
[2] L. Khaykovich *et al.*, Science **296**, 1290 (2002).
[3] Th. Anker *et al.*, Phys. Rev. Lett. **94**, 020403 (2005).
[4] M. Matuszewski *et al.*, Opt. Express **14**, 254 (2006).
[5] B. Eiermann *et al.*, Phys. Rev. Lett. **92**, 230401 (2004).
[6] T. J. Alexander, E. A. Ostrovskaya, and Yu. S. Kivshar, Phys. Rev. Lett. **96**, 040401 (2006).
[7] M. Rosenkranz *et al.*, Phys. Rev. A **77**, 063607 (2008).
[8] J. Wang *et al.*, Phys. Rev. A **79**, 043610 (2009).
[9] D. N. Neshev *et al.*, Phys. Rev. Lett. **99**, 123901 (2007).
[10] A. S. Desyatnikov *et al.*, Opt. Lett. **30**, 869 (2005).
[11] J. W. Fleischer *et al.*, Phys. Rev. Lett. **90**, 023902 (2003).
[12] G. L. Alfimov, V. V. Konotop, and M. Salerno, Europhys. Lett. **58**, 7 (2002).
[13] V. V. Konotop and M. Salerno, Phys. Rev. E **55**, 4706 (1997).